Electronic Supplementary Material (ESI) for Inorganic Chemistry Frontiers.
This journal is © the Partner Organisations 2024

Supporting Information

A universal Strategy of Constructing Cr-NiFe MOF/CMC Aerogel Composite Catalysts for Efficient Oxygen Evolution Reaction

Xin Yu[a], Jiangcheng Zhang[a], Yuxin Jia[a], Hu Yao[a], Baolian Su[b], Xiaohui Guo[a*]

[a]Key Lab of Synthetic and Natural Functional Molecule Chemistry of Ministry of Education, The College of Chemistry and Materials Science, Northwest University, Xi'an 710069, P. R. China.

[b]Department of inorganic chemistry, University of Namur, 61 rue de Bruxelles, B-5000 Namur, Belgium.

Key Laboratory, College of Materials and Science, Northwest University, Xi'an 710000, P.R. China

Experimental Procedure

Chemicals.

All reagents were used as purchased without further purification. Nickel nitrate hexahydrate ($Ni(NO_3)_2 \cdot 6H_2O$), ferric nitrate nonahydrate ($Fe(NO_3)_3 \cdot 9H_2O$), chromium nitrate nonahydrate ($Cr(NO_3)_3 \cdot 9H_2O$), Carboxymethyl cellulose (CMC), terephthalic acid ($C_8H_6O_4$), N-N dimethylformamide (C_3H_7NO), sodium hydroxide (NaOH), carbon paper (CP), potassium hydroxide (KOH) and acetone (C_3H_6O) were purchased from Aladdin's Reagent. were purchased from Aladdin reagent.

Electrocatalysts characterization.

The microscopic morphology and dimensions of the catalysts were obtained by field emission scanning electron microscopy (SEM, Hitachi SU8010) and field emission transmission electron microscopy (TEM, FEI Talos F200X). Scanning transmission electron microscopy (STEM) and X-ray energy dispersive spectroscopy (EDS) were characterized by microscopy using an energy disperser (HD2700) at 200 kV. The crystalline species and structures of the samples were characterised using a D8 Advance (Bruker) X-ray diffractometer (XRD) under Cu Kα radiation. X-ray photoelectron spectroscopy (XPS) was analysed by a PHI 5000 VersaProbeII instrument for the study of the elemental compositions and the chemical valence states of the surfaces. Fourier Transform Infrared Spectroscopy (FT-IR) employs infrared light as a light source to obtain infrared absorption spectra by scanning a specific range of wavelengths. FT-IR test is completed using Bruker's TENSOR27 infrared spectrometer.

Electrochemical measurements

Electrochemical tests were carried out using an electrochemical workstation (CHI 760) and measurements of cyclic voltammetry (CV) curves and linear scanning voltammetry (LSV) were carried out on Pt/C electrodes coated with catalyst. A measurement of the long-term corrosion resistance of carbon paper coated with a catalyst was conducted. The reference electrode and counter electrode were a Hg/HgO electrode and a Pt sheet, respectively. The working electrode was prepared by dispersing 1 mg of catalyst into a mixture containing 190 μL of ethanol and 10 μL of Nafion solution (5 wt%), and adding an appropriate amount of carbon black to enhance conductivity. The aforementioned solution was subjected to ultrasonication for a period of 1h. Subsequently, 8 μL of the catalyst ink was applied to the surface of the Pt/C electrode or carbon paper and allowed to dry naturally at room temperature. The mass loading of the catalyst was 0.16 mg/cm^2. The electrochemical testing was conducted in a 1 M KOH solution at a scan rate of 5 mV/s.

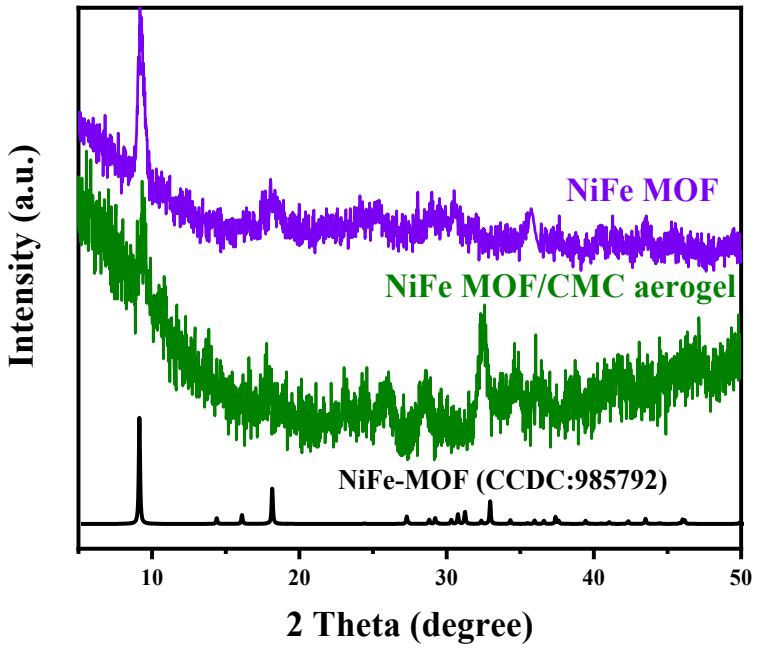

Fig. S1. XRD patterns of NiFe MOF and NiFe MOF/CMC aerogel.

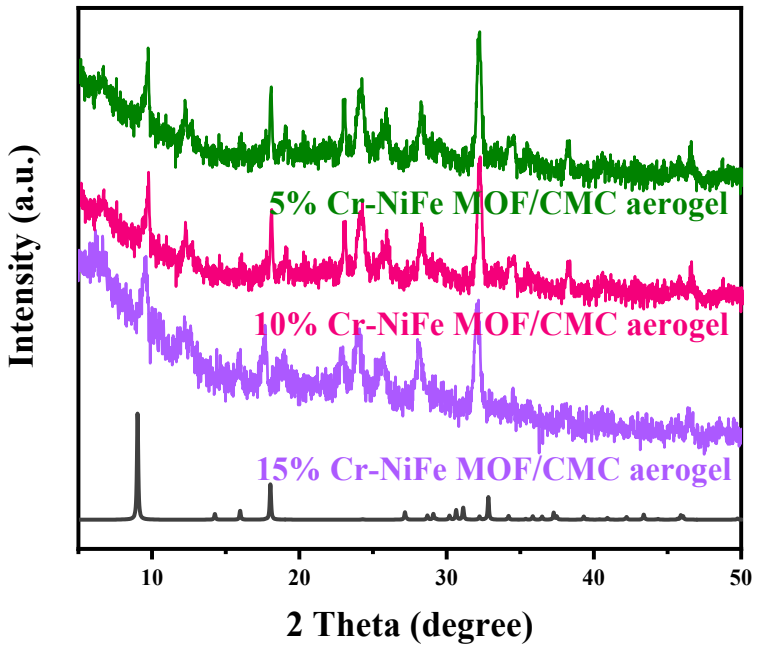

Fig. S2. XRD patterns of 5% Cr-NiFe MOF/CMC aerogel, 10% Cr-NiFe MOF/CMC aerogel and 15% Cr-NiFe MOF/CMC aerogel.

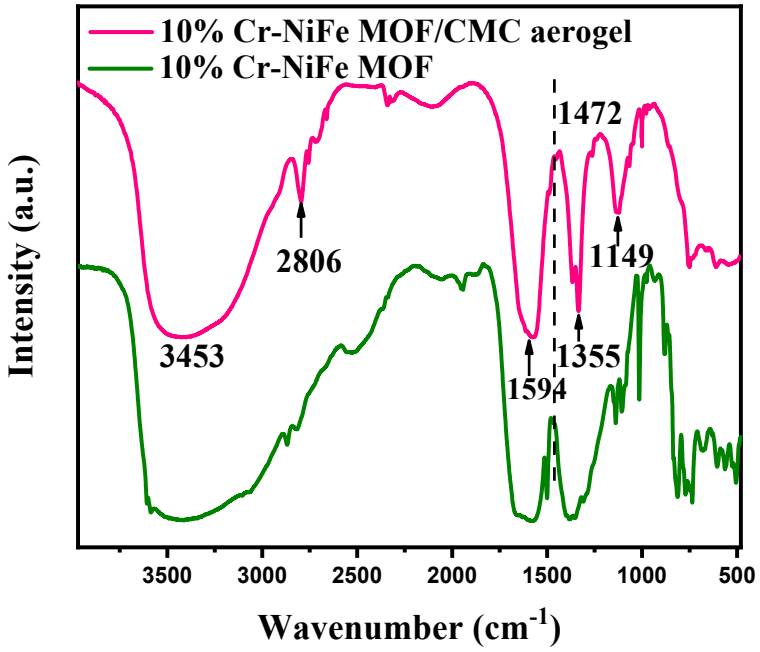

Fig. S3. Fourier transform infrared spectroscopy (FT-IR) of 10% Cr-NiFe MOF and 10% Cr-NiFe MOF/CMC aerogel.

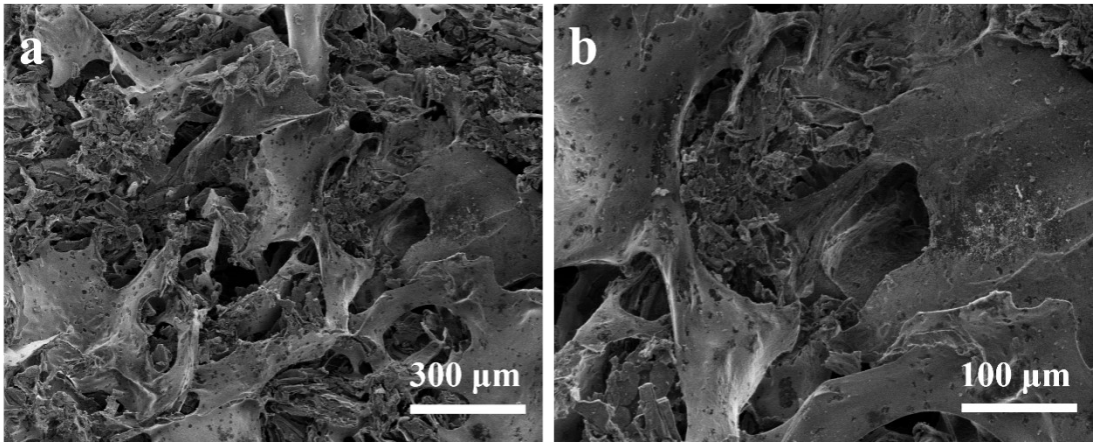

Fig. S4. (a-b) SEM of CMC aerogel with different magnifications.

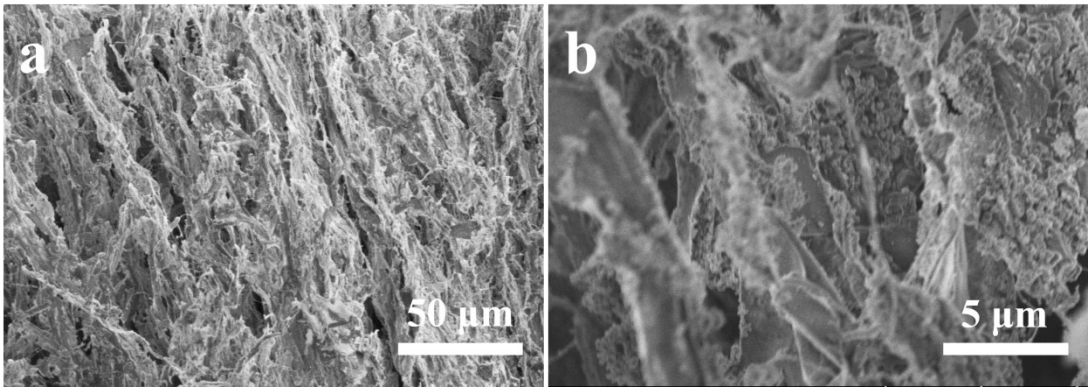

Fig. S5. (a-b) SEM of NiFe MOF/CMC aerogel with different magnifications.

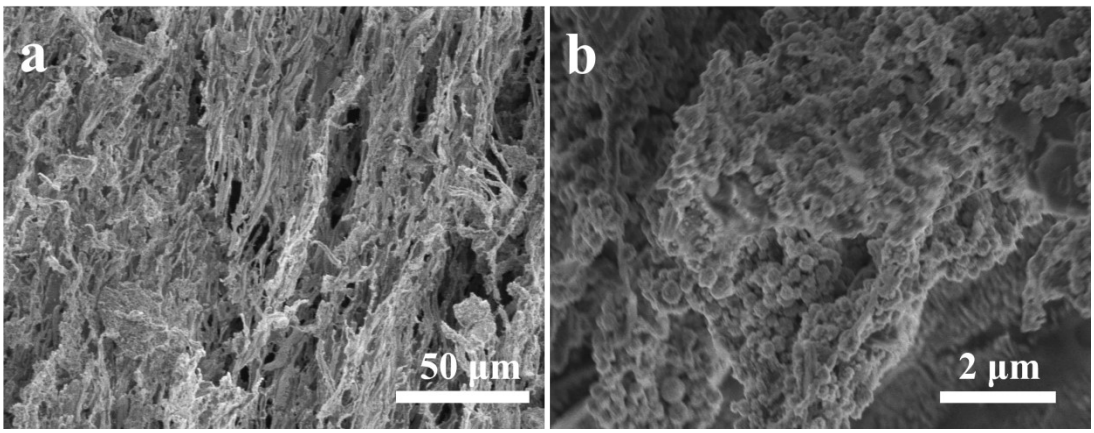

Fig. S6. (a-b) SEM of 5% Cr-NiFe MOF/CMC aerogel with different magnifications.

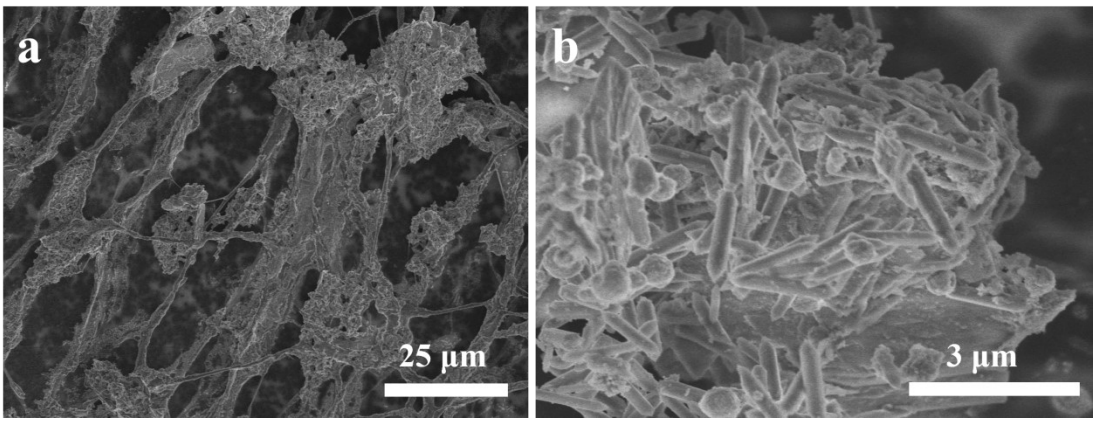

Fig. S7. (a-b) SEM of 10% Cr-NiFe MOF/CMC aerogel with different magnifications.

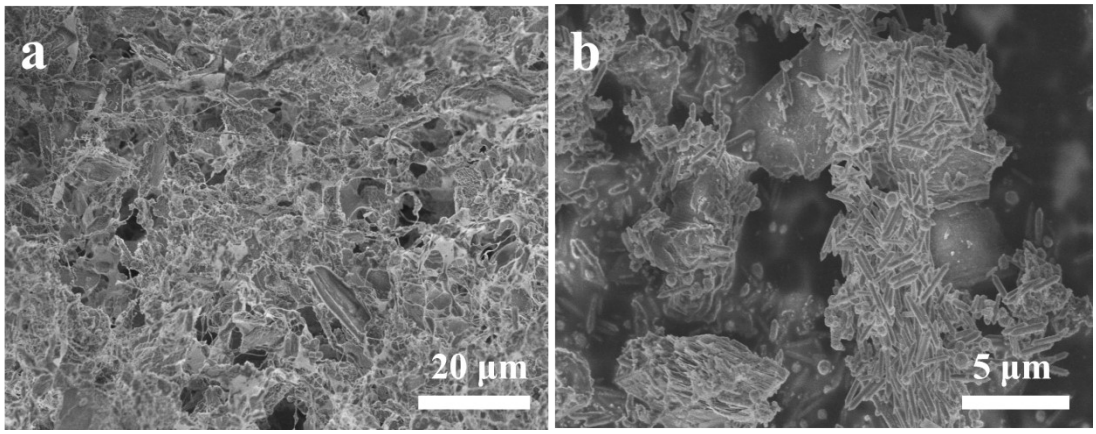

Fig. S8. (a-b) SEM of 15% Cr-NiFe MOF/CMC aerogel with different magnifications.

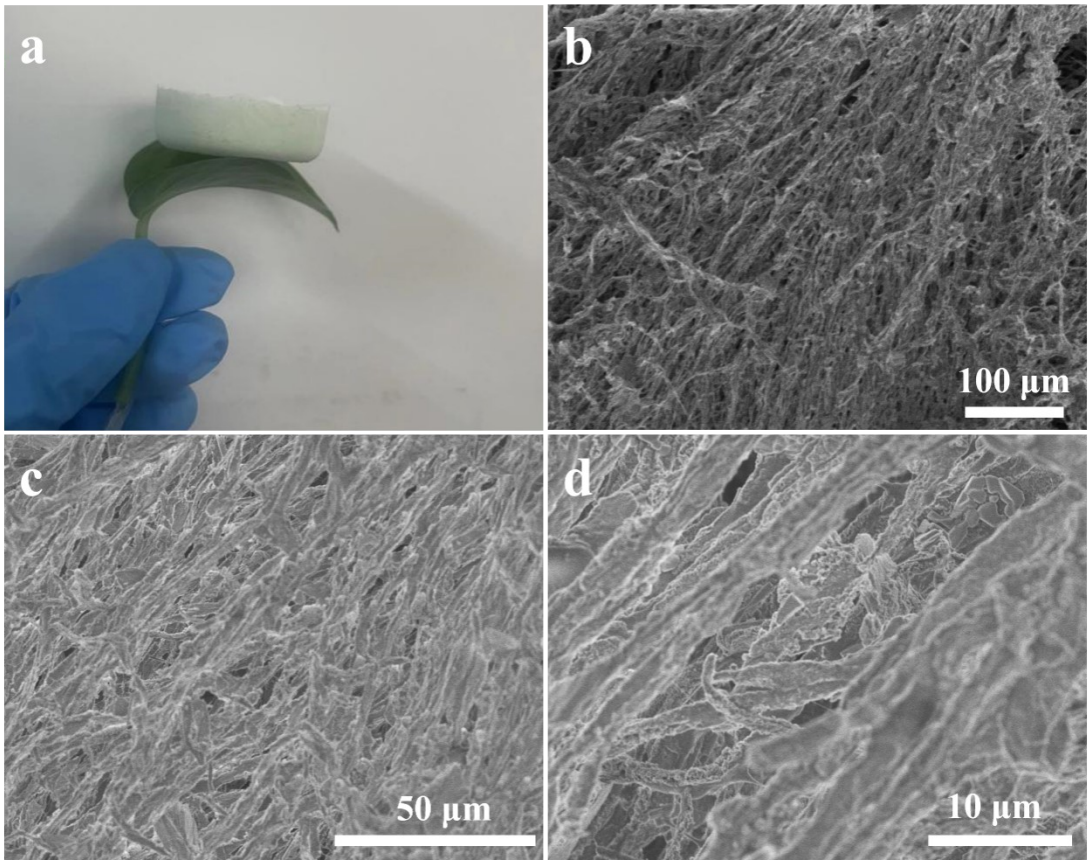

Fig. S9. (a) Optical photograph of the Ni MOF/CMC aerogel. (b-c) SEM of Ni MOF/CMC aerogel with different magnifications.

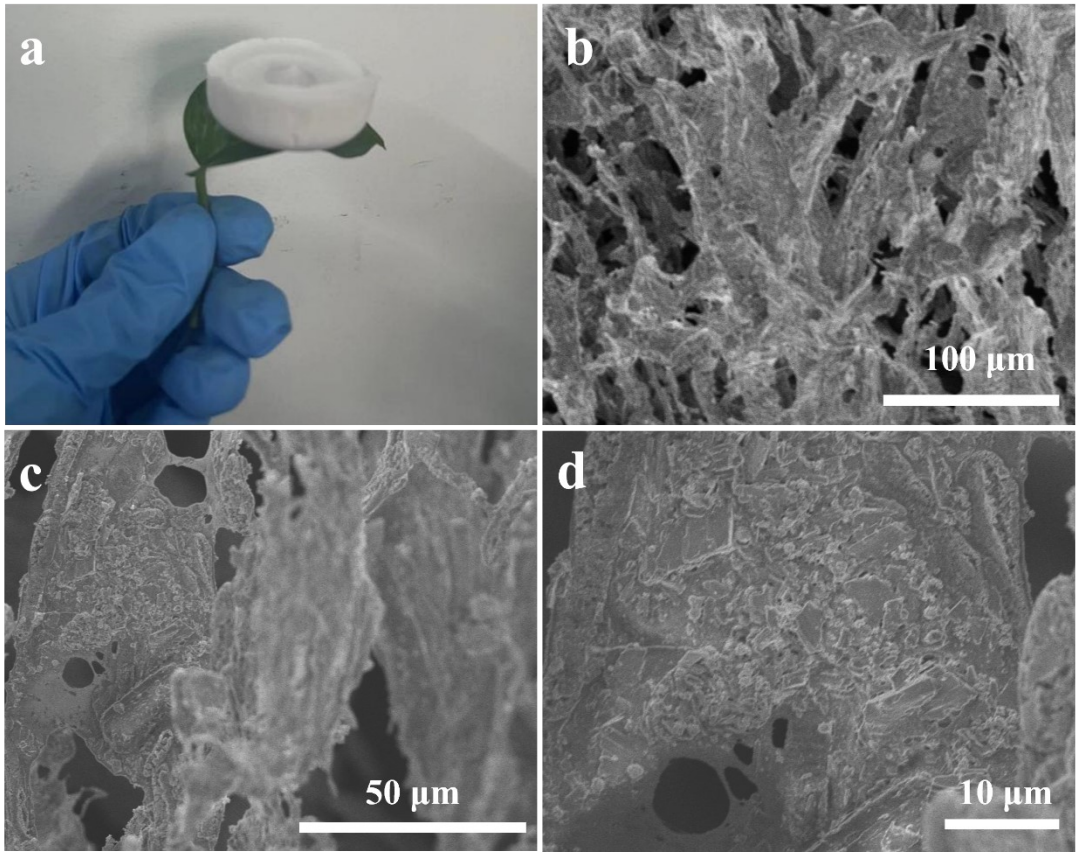

Fig. S10. (a) Optical photograph of the NiCo MOF/CMC aerogel. (b-c) SEM of NiCo MOF/CMC aerogel with different magnifications.

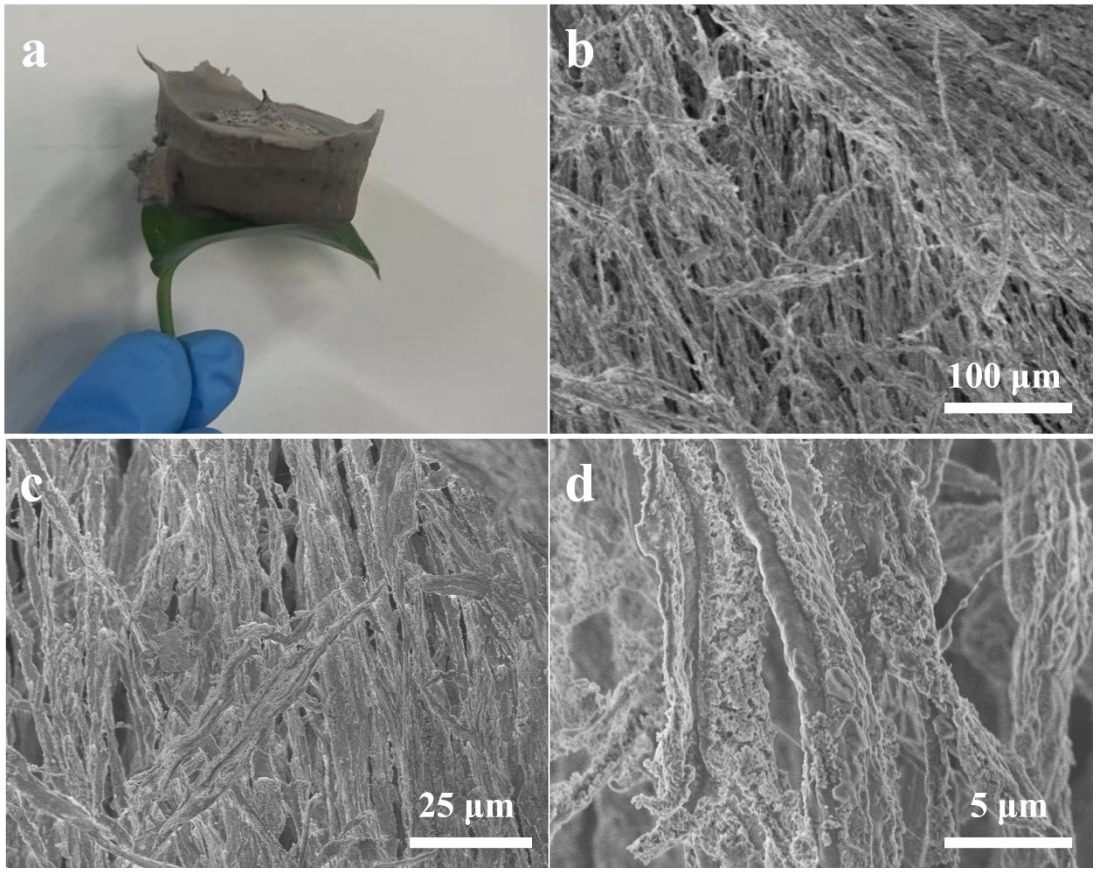

Fig. S11. (a) Optical photograph of the CoFe MOF/CMC aerogel. (b-c) SEM of CoFe MOF/CMC aerogel with different magnifications.

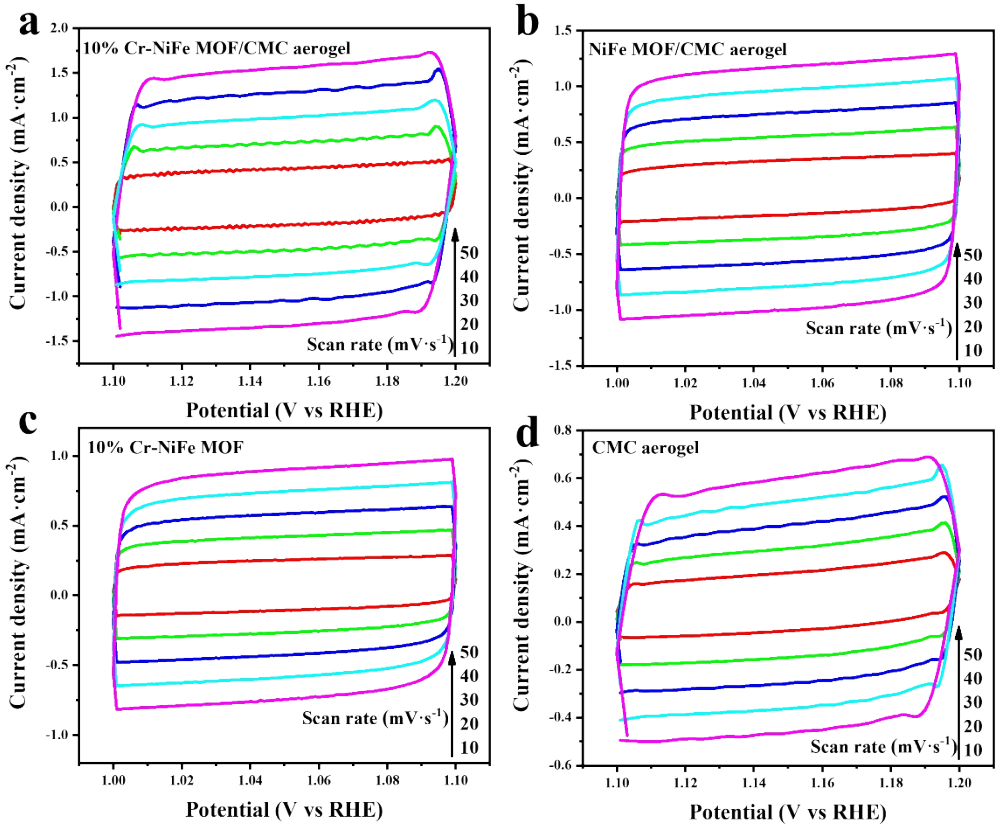

Fig. S12. CVs for (a) 10 % Cr-NiFe MOF/CMC aerogel, (b) NiFe MOF/CMC aerogel, (c) 10 % Cr-NiFe MOF, (d) CMC aerogel samples with different sweep speeds in the non-Faraday zone.

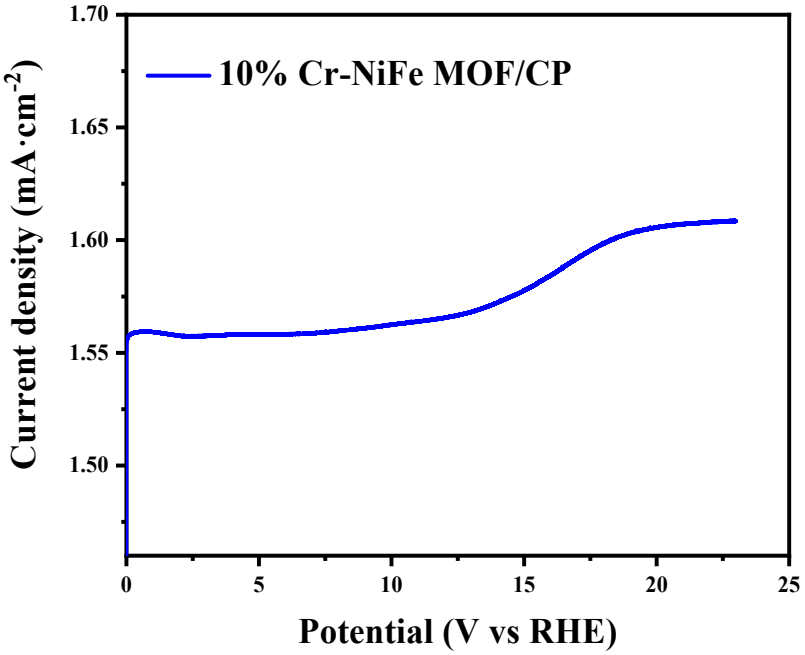

Fig. S13. Stability tests of 10% Cr-NiFe MOF/CP.

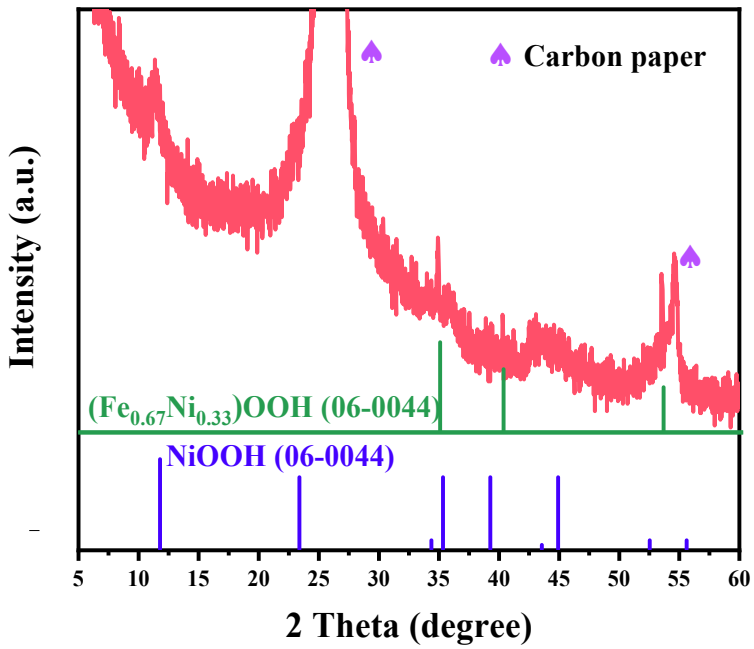

Fig. S14. XRD of 10% Cr-NiFe MOF/CMC aerogel after 210 h stability.

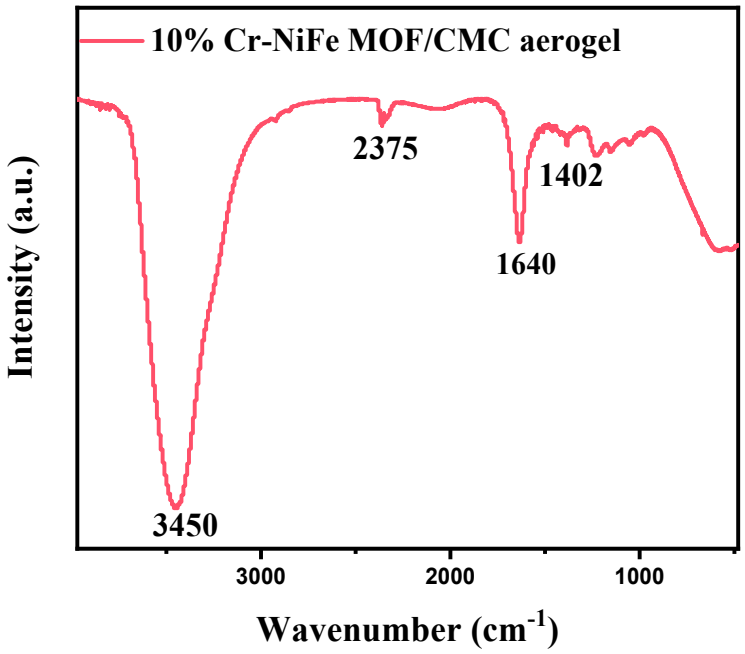

Fig. S15. FT-IR of 10% Cr-NiFe MOF/CMC aerogel after 210 h stability.

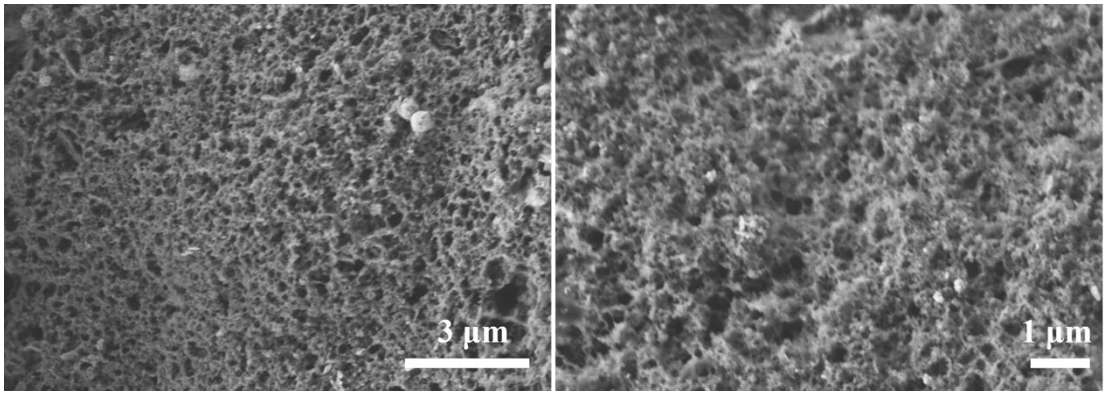

Fig. S16. SEM of 10% Cr-NiFe MOF/CMC aerogel after 1000 CVs with different magnifications.

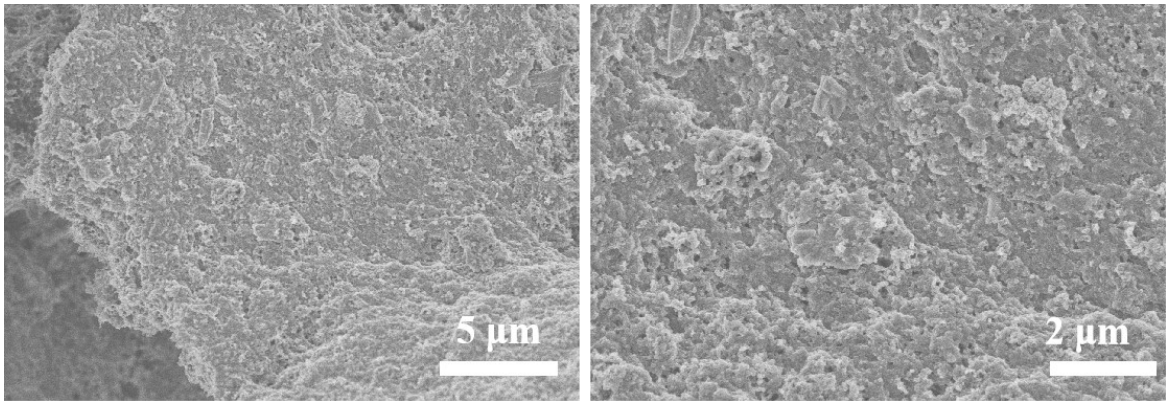

Fig. S17. SEM of 10% Cr-NiFe MOF/CMC aerogel after 210 h stability with different magnifications.

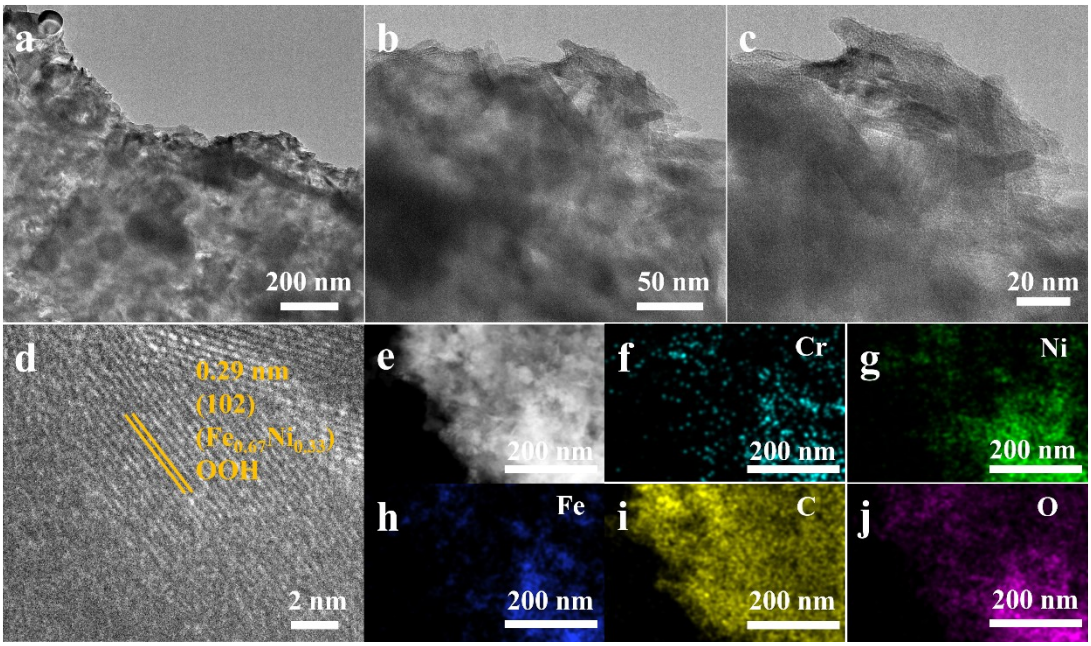

Fig. S18. 10% Cr-NiFe MOF/CMC aerogel after 210 h stability

(a-c) TEM images at varying magnifications. (d) HRTEM. (e) STEM-HADDF image. (f-j) Elements mapping images.

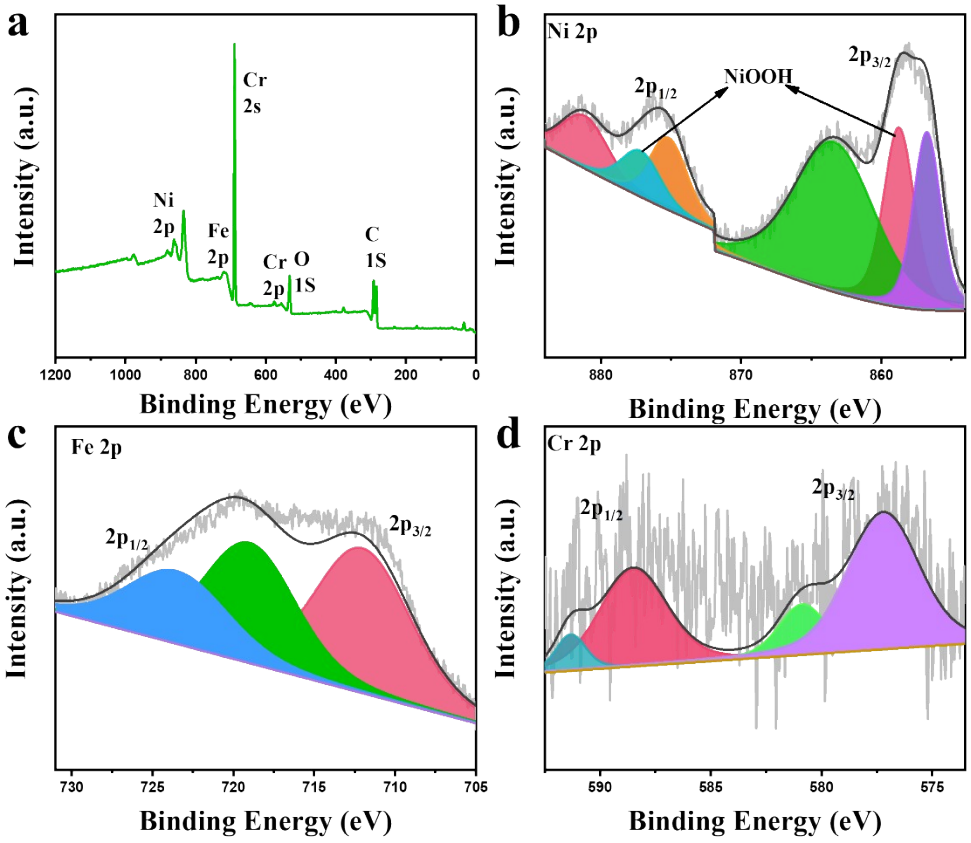

Fig. S19. The XPS characterizations of the 10% Cr-NiFe MOF/CMC aerogel after 210 h stability. (a) Survey XPS spectrum (b) Ni 2p (c) Fe 2p (d) Cr 2p.

Table 1. Catalytic activity of different aerogel or MOFs catalysts for OER

Catalyst	Overpotential (mV) @10 mA cm^{-2}	Tafel slope (mV dec^{-1})	Ref.
This work	235	53.7	/
Ni-Mo-P aerogel	235	96.6	[1]
Ru aerogel	237	81	[2]
Cu@Fe@Ni aerogel	240	47	[3]
Ni-SA@NC aerogel	280	89.8	[4]
Fe–Ni alloy carbon aerogel	260	60	[5]
$Co_{0.6}Fe_{0.4}$-MOF-74	280	56	[6]
Ni-MOF@Fe-MOF	265	82	[7]
Ni-MOFs	346	64	[8]
Co-Ni@HPA-MOF	320	58	[9]
Ru@NiCo-MOF-4	284	78.8	[10]
NiCo-MOF	310	106.3	[11]

References

[1] Zhang B, Yang F, Liu X, Wu N, Che S, Li Y. Phosphorus doped nickel-molybdenum aerogel for efficient overall water splitting. *Appl Catal B Environ. 2021;298:120494.*

[2] Yan S, Liao W, Zhong M, Li W, Wang C, Pinna N, et al. Partially oxidized ruthenium aerogel as highly active bifunctional electrocatalyst for overall water splitting in both alkaline and acidic media. *Appl Catal B Environ. 2022;307:121199.*

[3] Jiang B, Wan Z, Kang Y, Guo Y, Henzie J, Na J, et al. Auto-programmed synthesis of metallic aerogels: Core-shell Cu@Fe@Ni aerogels for efficient oxygen evolution reaction. *Nano Energy. 2021;81:105644*.

[4] Cheng Y, Guo H, Li X, Wu X, Xu X, Zheng L, et al. Rational design of ultrahigh loading metal single-atoms (Co, Ni, Mo) anchored on in-situ pre-crosslinked guar gum derived N-doped carbon aerogel for efficient overall water splitting. *Chem Eng J. 2021;410:128359.*

[5] Li H, Shu X, Tong P, Zhang J, An P, Lv Z, et al. Fe–Ni Alloy Nanoclusters Anchored on Carbon Aerogels as High-Efficiency Oxygen Electrocatalysts in Rechargeable Zn–Air Batteries. *Small. 2021;17:2102002.*

[6] Zhao X, Pattengale B, Fan D, Zou Z, Zhao Y, Du J, et al. Mixed-Node Metal–Organic Frameworks as Efficient Electrocatalysts for Oxygen Evolution Reaction. *ACS Energy Lett. 2018;3:2520-6.*

[7] Rui K, Zhao G, Chen Y, Lin Y, Zhou Q, Chen J, et al. Hybrid 2D Dual-Metal–Organic Frameworks for Enhanced Water Oxidation Catalysis. *Adv Funct Mater. 2018;28:1801554.*

[8] Maruthapandian V, Kumaraguru S, Mohan S, Saraswathy V, Muralidharan S. An Insight on the Electrocatalytic Mechanistic Study of Pristine Ni MOF (BTC) in Alkaline Medium for Enhanced OER and UOR. *ChemElectroChem. 2018;5:2795-807.*

[9] Lu M, Li Y, He P, Cong J, Chen D, Wang J, et al. Bimetallic metal-organic framework nanosheets as efficient electrocatalysts for oxygen evolution reaction. *J Solid State Chem. 2019;272:32-7.*

[10] Liu D, Xu H, Wang C, Shang H, Yu R, Wang Y, et al. 3D Porous Ru-Doped NiCo-MOF Hollow Nanospheres for Boosting Oxygen Evolution Reaction Electrocatalysis. *Inorg Chem. 2021;60:5882-9.*

[11] Liu Q, Chen J, Yang P, Yu F, Liu Z, Peng B. Directly application of bimetallic 2D-MOF for advanced electrocatalytic oxygen evolution. *Int J Hydrogen Energy. 2021;46:416-24.*